

Structural and optical modification of Ga-doped zinc oxide thin films induced by thermal annealing

Sandhya Negi^{1*}, Mahender Partap Singh Rana¹, Subodh K Gautam², R G Singh³, Fouran Singh² & R C Ramola¹

¹Department of Physics, HNB Garhwal University, Badshahi Thaul Campus, Tehri Garhwal 249 199, India

²Inter University Accelerator Centre, New Delhi 110 067, India

³Department of Physics, Bhagini Nivedita College, University of Delhi, New Delhi 110 043, India

Received 4 August 2014; revised 24 November 2014; accepted 18 February 2015

Ga doped ZnO (ZnO:Ga) thin films were prepared by the sol-gel spin coating technique. The films are annealed at different temperature varying from 500°C to 900°C in controlled oxygen environment. The effects of annealing temperature on structural, morphological and optical properties of films are investigated. The XRD results show that all deposited films are textured along the (101) direction and exhibits wurtzite phase of ZnO. The AFM images show that the grain size of ZnO films increased with increasing annealing temperature. Red shifting (band gap decreases) of the optical band gap is also observed on increasing the temperature. The observations are explained on the basis of stress and grain growth induced by thermal annealing.

Keywords: Gallium doped Zinc oxide, Zinc oxide thin film, Sol-gel spin coating, Thermal annealing Stress, Band Gap, Grain growth

1 Introduction

Zinc oxide (ZnO) is an *n*-type of semiconductor having wurtzite structure with many unique properties, such as a direct band gap of 3.37 eV and a large exciton binding energy of 60 meV. Its resistivity lies between 10^{-3} and 10^5 Ω -cm and shows the transparency in visible region. Due to these unique properties, ZnO is used in solar cells¹, gas sensors², transparent electrodes³, etc. Pure ZnO thin films are transparent but usually of low conductivity. Now a day, doping is the most important tool for the design and realization of ZnO based devices. When doping of elements, like aluminum, boron and gallium are introduced in it, then, its conductivity, transparency and crystal quality is improved⁴⁻⁸. Moreover, it is believed that the Ga, B, Al and In doped nanostructure are very important for diverse applications^{9,10}. Over these dopants, study of ZnO:Ga thin films became important in view of the fact that atomic radius of Ga is nearly equal to Zn, and hence, it easily substitutes Zn ions. Thus, less defects are generated as compared to other dopants. Further, Ga has greater electronegativity in comparison of aluminum. Therefore, Ga doped ZnO is more stable with respect to oxidation¹¹. Moreover, ZnO:Ga is less

studied area as compared to all the mentioned doped ZnO. The ZnO:Ga form a class of transparent conductive oxides (TCO) with important potential applications in solar cells, spintronic devices and window thermal coatings¹². Recent studies have shown the use of ZnO as an air stable anode in an OLED, providing additional evidence of ZnO:Ga thin film as a promising TCO for organic device applications¹³. Ga doped ZnO thin films are also useful in transparent electrode applications¹⁴.

There are a number of techniques employed for fabrication of ZnO thin films, such as chemical vapour deposition¹⁵, RF sputtering deposition¹⁶, pulse laser deposition¹⁷ and sol-gel^{18,19}. Sol-gel spin coating method has distinct advantage, such as low cost, simplicity, large area deposition and uniformity of film thickness²⁰. Thermal annealing is an important post growth treatment for modifying the ZnO films. It removes defects and thus, releases the internal stress²¹. So, in present investigation, effect of thermal annealing in oxygen environment on the structural and optical properties of ZnO:Ga (3 at.%) thin films is studied.

2 Experimental Procedure

Ga doped ZnO (ZnO:Ga) thin film were deposited on silica substrate by sol-gel method using spin

*Corresponding author (E-mail: sandhyanegi@gmail.com)

coating technique. Zinc acetate dehydrate $\text{Zn}(\text{CH}_3\text{COO})_2 \cdot 2\text{H}_2\text{O}$ was used as a starting material; and 2-methoxyethanol and diethylamine (DEA) were used as solvent and stabilizer, respectively. The ZnO precursor solution was prepared by dissolving zinc acetate dehydrate in 2-methoxyethanol. The total concentration of the sol was maintained at 0.5 mol L^{-1} , then DEA was dissolved in to the solution. The molar ratio DEA/Zn was fixed at 1.0. The Gallium nitrate was dissolved in the solution to obtain ZnO:Ga solution. Gallium concentration was fixed at 3 at.%. The mixture solution was stirred at 60°C for 2 h. The transparent and homogenous solution was obtained after 72 h. The solution was then spin coated on silica substrate at 2800 rpm. After deposition, the films were dried in air at 220°C temperature for 10 min over hot plate to evaporate the solvent and organic residuals. The process of coating and drying at 220°C temperature was repeated 10-12 times in order to get a film of desired thickness. Finally, all the deposited films are annealed in presence of air at 400°C temperature. Now, these deposited films were thermal annealed at 500°C , 700°C , and 900°C temperature for 1 h in oxygen environment using microprocessor controlled furnace.

Structural analysis was carried out by using glancing angle X-ray diffraction (GAXRD) patterns obtained from Bruker D8 Advanced XRD machine. The surface morphology of doped and undoped films were studied using the Nano Scope IIIa SPM atomic force microscopy (AFM) and band gap of film was measured by optical absorption using Hitachi (UV-3300) double beam spectrophotometer. The flow chart of procedure for preparing ZnO:Ga films is shown in Fig. 1.

3 Results and Discussion

The results of structural and the optical measurements performed on the ZnO:Ga (3 at.%) films annealed at different temperature are presented here.

3.1 Structural analysis

Figure 2 shows the Glancing angle X-ray diffraction (GAXRD) pattern of ZnO:Ga films. The GAXRD results reveal that the ZnO:Ga thin films are of good crystalline quality and polycrystalline in nature. A texturing along (101) axis can be seen in all ZnO:Ga thin films annealed at $500\text{--}900^\circ\text{C}$ temperature. The diffraction intensity of the (101) peak increases with the increase of

annealing temperature up to 900°C . The increase of peak intensity with increasing annealing temperature is due to improvements of the stoichiometry of the film and the crystallite quality. The average crystallite size (D) is also estimated from XRD data using Scherrer's formula²²:

$$D = \frac{0.9\lambda}{\beta \cos \theta} \quad \dots (1)$$

where, β , is full width at half maximum (FWHM) in radian; λ , wavelength of X-ray (1.5406 \AA for Cu- K_α); and θ , Bragg angle. The crystallite size is calculated for (101) diffraction peak and given in Table 1. It is clear from the calculated crystallite size

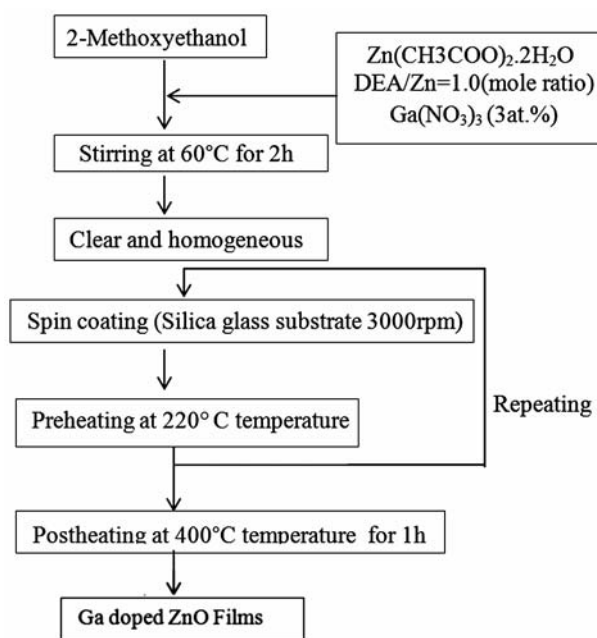


Fig. 1 — Flow chart showing the procedure for preparing ZnO:Ga films

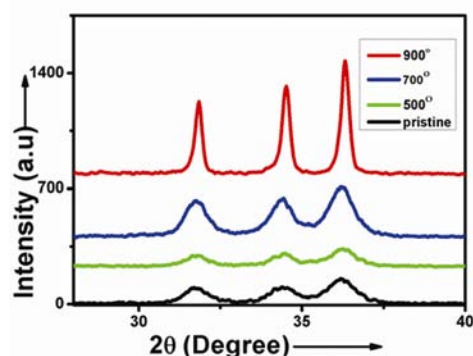


Fig. 2 — XRD patterns of ZnO:Ga thin films with different annealing temperatures

that crystallite size increases with annealing temperature. The crystallite size of ZnO:Ga thin films increases rapidly from 8.4 nm to 33 nm with increasing the annealing temperature from 500°C to 900°C. The lattice parameters 'a' and 'c' of films are calculated from the diffraction peaks (002) and (101) using the relation for hexagonal structure of ZnO:

$$d_{hkl} = \frac{1}{\sqrt{\frac{4(h^2 + hk + k^2)}{3a^2} + \frac{i^2}{c^2}}} \quad \dots (2)$$

where, value of d_{hkl} is determined using the Bragg condition in the Bragg's law:

$$2d_{hkl} \sin \theta = \lambda \quad \dots (3)$$

where θ is Bragg's angle; and λ is wavelength of Cu-K α line (0.15406 nm).

The obtained value of lattice constant a and c , c/a ratio is tabulated in Table 1. The value of c/a of ZnO:Ga thin film is very close to the value of 1.633, which is the ideal value for an hcp structure^{23,24}. The

Table 1 — Average crystallite size and lattice parameters of ZnO:Ga films with different annealing temperatures

Temperature (°C)	Avg crystallite size (nm)	Lattice constant		c/a ratio	Stress (Pa)
		a (Å)	c (Å)		
Pristine	8.40	3.247	5.208	1.603	-8.95×10^{-7}
500	9.49	3.244	5.212	1.606	-2.68×10^{-8}
700	10.34	3.238	5.206	1.607	0
900	33.00	3.238	5.192	1.603	$+6.26 \times 10^{-8}$

value of stress in the films is also calculated using the formula²⁵:

$$\sigma = -233 \times 10^9 \left[\frac{c - c_0}{c_0} \right] \text{ Pa} \quad \dots (4)$$

where σ is stress; c is lattice parameter of the film; and c_0 is strain free lattice parameter, which is 0.5206 nm. It is found that pristine sample have a stress of compressive nature, which changes from compressive to tensile nature when annealing temperature reaches to its highest value (900°C). The calculated values of stress are shown in Table 1. Generally, when thin films are deposited over a substrate, deposited films get stressed due to the presence of structural defect. It is a well reported fact that stress gradually decreases with increasing annealing temperature^{21,26-28}. In present work, thermal annealing at 500°C removes such defect from pristine film and thus, reduced film's stress. Here, it is to be noted that film annealed at 500°C has some stress because of some defect that are still present in film. So, further annealing at higher temperature 700°C removes all such presented defects in film, which couldn't annealed at lower temperature and thus, makes the film completely stress free.

3.2 Morphological studies

The surface morphology of the annealed ZnO:Ga thin films are studied using atomic force microscope (AFM). The 3D images of pristine film and 900°C annealed film are shown in Fig. 3. The average grain size measured from AFM is 40 nm for pristine film

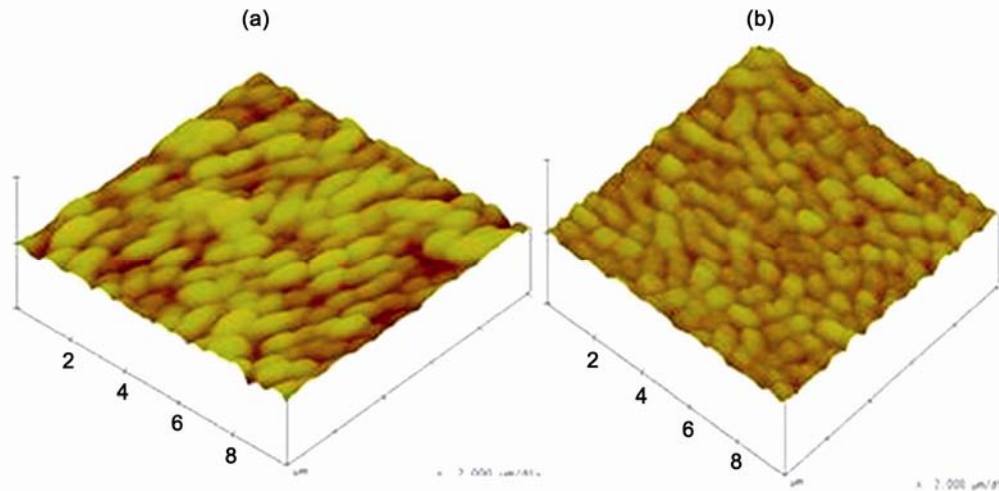


Fig. 3 — AFM images of ZnO:Ga (3at.%) films: (a) 3D image of pristine ZnO:Ga film and (b) 3D image of ZnO:Ga film at 900°C

and 89 nm for the film annealed at 900°C temperature, which are much larger than that calculated from XRD. It may be because the grain size, measured from AFM, is the surface morphology of coalesced grains²¹. The coalescence of grains during the annealing process is because high temperature stimulates the migration of grain boundaries²⁹, thus, the grain size increases with temperature. The roughness for the pristine film was 9 nm and for annealed film at 900°C temperature, it was 14 nm, which shows the increment in roughness with increasing temperature. It is due to the fact that major grain growth yields an increase in the surface roughness³⁰.

3.3 Optical studies

Optical transmittance spectra in the wavelength range of 200-800 nm of ZnO:Ga thin film at different temperature series is shown in Fig. 4. The transmittance lies in the visible region of 400 - 800 nm for all films. Sharp absorption edge of all films is located near 380 nm, which is due to the fact that ZnO is a direct band gap semiconductor³¹. Transmittance of films decreases with increasing annealing temperature as shown in Table 2. The decrease in the transmittance may be due to increasing optical scattering caused by increment of roughness as determined by the AFM³². The optical band gap is calculated using Tauc's plot methods³³:

$$ahv = B (hv - E_g)^{1/2} \quad \dots (5)$$

where a is the absorption coefficient; and hv is the photon energy of ZnO:Ga thin films. Figure 5 shows the Tauc's plots of the pristine and annealed

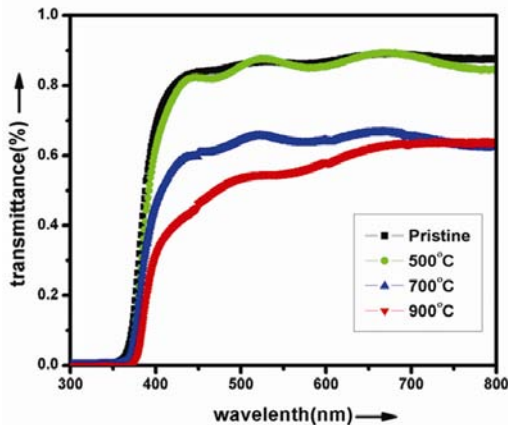


Fig. 4 — Optical transmittance spectra of ZnO:Ga films with different temperatures

samples. It is observed that band gap of the pristine film is around 3.30 eV, which decreases continuously with increasing annealing temperature. The band gap of thin film depends on stress, grain size and carrier concentration. It is clear from the values of stress, calculated from XRD data, that initially, it has a compressive nature, which decreases with annealing of the films and films become completely stress free at 700°C. At highest annealing temperature (900°C), stress turns into tensile nature. It is a well reported fact that compressive stress causes a blue shift and tensile stress causes a red shift in the band gap³⁴. In this case, initial thermal annealing temperatures (up to 700°C) removes the compressive stress and band gap tends to normalize. At highest temperature, band gap decreases further due to change in nature of stress from compressive to tensile. Another explanation of the observed modification in the band gap is based on grain growth. Grain growth causes a red shift in band gap³⁵. XRD and AFM data shows that there is an increase in grain size with increasing annealing temperature. So, it can be inferred that grain growth causes red shift in band gap. Therefore, both stress and grain growth are jointly responsible for the observed red shift in the band gap of ZnO:Ga thin films.

Table 2 — Transmittance and optical band gap of ZnO:Ga films with different annealing temperatures

Temperature (°C)	Transmittance (%)	Band gap (eV)
Pristine	85	3.30
500	84	3.28
700	65	3.27
900	62	3.24

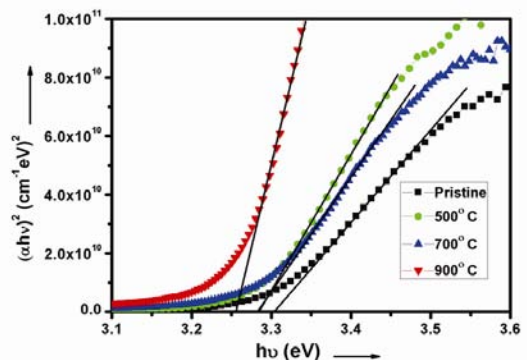


Fig. 5 — Tauc's plot of ZnO:Ga thin films showing the red shift of band gap with increasing annealing temperature

4 Conclusions

Ga doped thin films were synthesized by sol-gel technique. XRD results show the texturing along (101) axis of ZnO:Ga films annealed at different temperature from 500°C to 900°C. The crystallite size increases with increasing annealing temperature. AFM results reveal that grain size and roughness of films increases with increasing annealing temperature. All films shows transparency in the entire visible region. The band gap of annealed ZnO:Ga films is red shifted, which can be explained by grain growth and stress induced by thermal annealing.

Acknowledgment

The authors are thankful to Inter University Accelerator Centre, New Delhi for providing thin film synthesis and characterization facilities such as, XRD, UV-visible and AFM. One of the authors (SN) is also thankful to UGC for providing the financial support under the scheme of Ph. D. fellowship.

References

- Rao A R & Dutta V, *Nanotechnology*, 19 (2008) 445712.
- Suceha M, Christoulaki S, Moschovis K, Katsarakis N & Kiriakidis G, *Thin Solid Film*, 515 (2006) 551.
- Lin C C, Chu B T T, Tobias G, Sahakalken S, Roth S, Green M L H & Chen S Y, *Nanotechnology*, 20 (2009) 105703.
- Lee J H & Park B O, *Thin Solid Film*, 426 (2003) 94.
- Kumar V, Singh R G, Purohit L P & Mehra R M, *J Mater Sci Technol*, 7 (6) (2011) 481.
- Nayak P K, Yang J, Jinwoo K, Chung S, Lee J & Hong Y, *J Phys D Appl Phys*, 42 (2009) 035102.
- Bhosle V, Tiwari A & Narayan J, *Appl Phys Lett*, 88 (2006) 032106.
- Merchant J D & Cocivera M, *Chem Mater*, 7 (1995) 1742.
- Zhong J, Muthukumar S, Chen Y, Lu Y, Ng H M, Jiang W & Garfunkel E L, *Appl Phys Lett*, 83 (2003) 3401.
- Kim H, Gilmore C M, Horwitz J S, Pique A, Murata H, Kushto G P, Schlaf R, Kafafi Z H & Chrisey D B, *Appl Phys Lett*, 76 (2000) 259.
- Yim K, Kim H W & Lee C, *Mater Sci Technol*, 23 (2007) 108.
- Hanada T, *Basic properties of ZnO, GaN and related materials*, edited by Yao T & Hong S K (Springer, Berlin), 2009, 1.
- Bolink H J, Coronado E, Repetto D & Sessolo M, *Appl Phys Lett*, 91 (2007) 223501.
- Kim C E, Moon P, Yun I, Kim S, Myoung J M, Jang H W & Bang J, *Expert Syst Appl*, 38 (2011) 2823.
- Funakubo H, Mizutani N, Yonetsu M, Saiki A & Shinozaki K, *J Electroceram*, 4 (1999) 25.
- Minami T, Nato H & Takata S, *Appl Phys Lett*, 41 (1982) 958.
- Ardakani H K, *Thin Solid Films*, 287 (1996) 280.
- Ohyama M, Kouzuka H & Yoka T, *Thin Solid Films*, 306 (1997) 78.
- Natsume Y & Sakata H, *Thin Solid Films*, 372 (2000) 30.
- Bringer C J & Scherer G W, *Sol-gel science: The physics and chemistry of sol-gel processing*, (Academic Press Inc, Sandiago, CA), 1990.
- Singh R G, Singh F, Kumar V & Mehra R M, *Appl Phys*, 11 (2011) 624.
- Cullity B D, *Element of X-ray diffraction*, (Eddission Wesley, MA, London), 1978, 284.
- Ozgun U, Alivov Y I, Liu C, Teke A, Reshchikov M A, Dogan S, Avrutin V, Cho S J & Morkoc H, *J Appl Phys*, 98 (2005) 041301.
- Abrahams S C & Berstein J L, *Actacryst B*, 25 (1969) 1233.
- Chen M, Pei Z I, Sun C, Wen L S & Wang Z, *J Cryst Growth*, 220 (2000) 254.
- Shan F K, Kim B I, Liu G X, Shon J Y, Lee W J, Shin B C & Yu Y S, *J Appl Phys*, 95 (2004) 4772.
- Tripathi N & Rath S, *J Solid State Sci Technol*, 3 (2014) 21.
- Bender M, Seelig W, Dube C, Frankenberger H, Ocker B & Stollenwerk J, *Thin Solid Film*, 326 (1998) 72.
- Lin B, Xiao Z, Sun X, Guo S S, Wu J, Wu R & Liu J, *Jpn J Appl Phys*, 45 (2006) 7860.
- Agarwal D C, Singh F, Kabiraj D, Sen S, Kuleriya P K, Sulania I, Nojaki S, Chouhan R S & Avasthi D K, *J Phys D Appl Phys*, 41 (2008) 045305.
- Saleem M, Fang L, Wakeel A, Rashad M & Kong C Y, *World J Condens Matter Phys*, 2 (2012) 10.
- Lou X, Shen H, Zhang H & Li B, *Nonferrous Met Soc China*, 17 (2007) 814.
- Szczyrbowski J, Dietrich A & Hoffmann H, *Physica Status Solidi A*, 78 (1983) 243.
- Mahmood A, Ahmed N, Raza Q, Khan T M, Mehmood M, Hasan M M & Mahmood N, *Phys Scr*, 82 (2010) 065801.
- Shana M B, Sudakar C, Setzler G, Dixit A, Thakur J S, Lawes G, Naik R, Naik V M & Vaishnawa P P, *App Phys Lett*, 93 (2008) 231909.